Advances in Materials Research, *Vol. 12, No. 1 (2023) 1-13*
https://doi.org/10.12989/amr.2023.12.1.001

Effect of cobalt ferrite on curing and electromagnetic properties of natural rubber composites

Anuchit Hunyek[1a] and Chitnarong Sirisathitkul*[2,3]

[1]*Program of General Education-Science (Physics), Faculty of Liberal Arts, Rajamangala University of Technology Rattanakosin, Wangklaikangwon Campus, Prachuap Khiri Khan, Thailand*
[2]*Division of Physics, School of Science, Walailak University, Nakhon Si Thammarat, Thailand*
[3]*Functional Materials and Nanotechnology Center of Excellence, Walailak University, Nakhon Si Thammarat, Thailand*

(Received August 24, 2021, Revised April 6, 2022, Accepted April 12, 2022)

Abstract. The combination of cobalt ferrite and natural rubber has a potential to enhance the functional properties of rubber ferrite composites available on the market. In this study, cobalt ferrite was synthesized by the sol-gel method with tapioca starch as a cheating agent and then incorporated into natural rubber using an internal mixer. The curing characteristics, magnetic hysteresis, complex permeability, and permittivity of the rubber ferrite composites were studied as a function of the loading from 0 to 25 phr. The cure time and scorch time tended to reduce with the addition of non-reinforced cobalt ferrite fillers. The remanent and saturation magnetizations were linearly proportional to the cobalt ferrite loading, consistent with the rule of mixture. On the other hand, the increase in cobalt ferrite loading from 5 to 25 phr slightly affected the coercive field and the complex permeability. Using the maximum loading of 25 phr, both real and imaginary parts of the permittivity were significantly raised and reduced with the frequency in the 10-300 MHz range.

Keywords: cobalt ferrite; curing; magnetic hysteresis; natural rubber; rubber ferrite composite

1. Introduction

Attentions in cobalt ferrite ($CoFe_2O_4$) have considerably been raised in the past few years by the reports of its inclusion in functional core-shell structures and composites (Mmelesi *et al.* 2021, Zeng *et al.* 2021). Electromagnetic properties are already implemented in a bulk form, and cobalt ferrite nanoparticles have numerous biomedical and environmental applications as reviewed in the literatures (Jauhar *et al.* 2016, Srinivasan *et al.* 2018). Composite productions allow opportunities to combine its remarkable characteristics with the outstanding properties of other materials. Based on electromagnetic wave absorption by spinel ferrites, composites for radio frequency (RF) and microwave shielding were proposed by combining with carbon in the forms of graphite (Ismail *et al.* 2019), carbon nanotube (Wang *et al.* 2019) and graphene (Zhang *et al.* 2019). Recently, a

*Corresponding author, Associate Professor, E-mail: schitnar@mail.wu.ac.th
[a]Ph.D., E-mail: anuchit.hun@rmutr.ac.th

http://www.techno-press.org/?journal=amr&subpage=5 ISSN: 2234-0912 (Print), 2234-179X (Online)

composite was prepared by spin-coating cobalt ferrite on porous silicon (Kalifa *et al.* 2020). From cobalt ferrite-barium titanate multiferroic nanocomposites, the product properties were obtained (Mahalakshmi *et al.* 2019) and magnetoelectric sensors were developed (Kumar *et al.* 2020, Shariati *et al.* 2020).

To fabricate functional composites, polymers possess mechanical properties and weight suitable for embedding particulate fillers. However, different fillers affect the structures and properties of polymer composites (Garigipati and Malkapuram 2020, Kalmagambetova and Bogoyavlenskaya 2021). Besides, composite properties are regulated by interfaces between filler and matrix (Wang *et al.* 2021a). Assorted properties were obtained by filling cobalt ferrites in various polymeric matrices, including polyurethane (Hunyek *et al.* 2013), polypropylene (Hunyek *et al.* 2019), and epoxy resin (Yang *et al.* 2021). The mechanical properties of cobalt ferrite-epoxy composites were improved by adding silica as co-fillers (Megahed *et al.* 2021). Biodegradable composites composed of cellulose, polyaniline, and cobalt ferrite nanoparticles were developed for electromagnetic applications (Abou Hammad *et al.* 2019). Furthermore, cobalt ferrite and polyaniline were included in composites developed for supercapacitor electrodes (Das and Verma 2019).

For this study, natural rubber is selected to combine with cobalt ferrite because of its distinct elastic properties and local availability in many countries. Rubber ferrite composites are easily processed with a high commercial production rate. The products based on synthetic rubbers and other ferrites in the market are implemented as flexible magnets and electromagnetic wave absorbers. The functionality of cobalt ferrite and the benefits of natural rubber previously described can enhance the demands of rubber ferrite composites. In forms of environmental-friendly composites, the product can be extended to other applications of cobalt ferrite, including the removal of dyes and heavy metal ions (Shapkin *et al.* 2020). The loadings used in this study are 5-25 phr (part per hundred rubber) because it was reported that the mechanical properties of natural rubber were severely degraded by the ferrite loadings of 30 phr and over (Malini *et al.* 2003). The study on the effects of the cobalt ferrite loading on curing, dielectric, and magnetic properties provides essential information for commercial production of this rubber ferrite composite in the future.

2. Materials and methods

2.1 Preparation and characterization of cobalt ferrite

Natural rubber Cobalt ferrite powders were obtained from a chemical reaction between iron nitrate (Sigma Aldrich, 99.95%) and cobalt nitrate (Sigma Aldrich, 99.90%). Following the procedure detailed in the literature (Hunyek *et al.* 2017), tapioca starch was used as a cheating agent instead of sago starch. Tapioca starch was slowly dissolved in deionized water at a weight/volume of 3:20 under constant stirring. Cobalt nitrate ($Co(NO_3)_2 \bullet 6H_2O$) and iron nitrate $Fe(NO_3)_3 \bullet 9H_2O$ powders were then added to the solution in a weight/volume ratio of 1:4. The solution with increasing viscosity was continuously stirred at 80°C for 10-12 h until turning into the gel. The weight and derivative weight loss of the sol-gel derived product were measured by thermogravimetry (TGA, Perkin Elmer TGA7) up to 1000°C. To enhance the crystalline cobalt ferrite phase, the dried product was calcined for 10 h at the temperature determined by TGA. The phase was confirmed by X-ray diffractometry (XRD, Philips X'Pert MPD).

Table 1 Formulation of the mixes for preparing cobalt ferrite-natural rubber composites

Sample code	Materials (phr)						
	NR (ADS)	Stearic Acid	ZnO	ZMP	CBS	Sulphur	Cobalt Ferrite
NR00CF	100	1	5	1	0.6	1.5	0
NR05CF	100	1	5	1	0.6	1.5	5
NR10CF	100	1	5	1	0.6	1.5	10
NR15CF	100	1	5	1	0.6	1.5	15
NR20CF	100	1	5	1	0.6	1.5	20
NR25CF	100	1	5	1	0.6	1.5	25

2.2 Preparation and characterization of cobalt ferrite-natural rubber composites

Sol-gel derived cobalt ferrites were incorporated into natural rubber using an internal mixer machine at temperatures between 90 and 100°C for 1 min. Six samples were prepared with varying cobalt ferrite loadings from 0 to 25 phr and other ingredients as listed in Table 1. As an exception, sulphur was subsequently added to the compound rubber using a two-roll mill. The sulphur vulcanization is accelerated by the ZnO addition, which also improves the rubber compound properties. The vulcanization behaviors of rubber ferrite composites were examined by oscillating disk rheometer (ODR, TECH PRO rheoTECH OD+) to find the cure time used for forming the product by compression molding. After their cure properties were determined, all composites were hot-pressed in a hydraulic compression mold.

The morphology of the composites was inspected by scanning electron microscopy (SEM, JEOL JSM6301F), and their magnetic properties were characterized by a vibrating sample magnetometer (VSM). Both complex permittivity and permeability were measured as a function of frequency from 10 to 1000 MHz by an impedance/material analyzer (Agilent 4291B).

3. Results and discussion

3.1 Thermal and phase analyses

The weight percent and derivative weight loss from TGA are shown in Fig. 1. After the initial slight weight loss by removing adsorbed water (Mirzaee *et al.* 2014), the thermal behaviors of the sol-gel product are divided into three regimes. Up to 550°C, the gradual weight loss was approximately 23% of the initial weight. In the middle range from 550 to 600°C, a sudden weight loss of 12% occurs, resulting in a sharp drop in the derivative weight loss curve. Similar observations were attributed to the decomposition of starch (Ojogbo *et al.* 2018, Paluch *et al.* 2022) and other residual organic compounds (Mustafa *et al.* 2015). The further increase in temperature over 600°C in the last regime only slightly changes the weight of the sol-gel product since the crystalline spinel ferrite has been formed (Mustafa *et al.* 2015). These variations, related to the decomposition and phase transformation, can be used to determine the temperature for the calcination as 600°C.

The phase of sol-gel derived product is identified by an XRD pattern in Fig. 2. Characteristic peaks at an angle of 30.1°, 35.4°, 37.0°, 43.0°, 53.4°, 56.9°, and 62.6° respectively correspond to

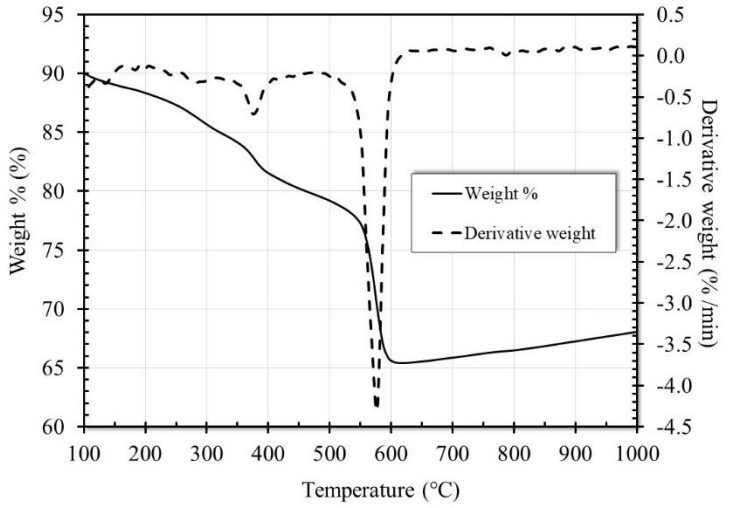

Fig. 1 TGA curves of the sol-gel derived product from 100 to 1000°C

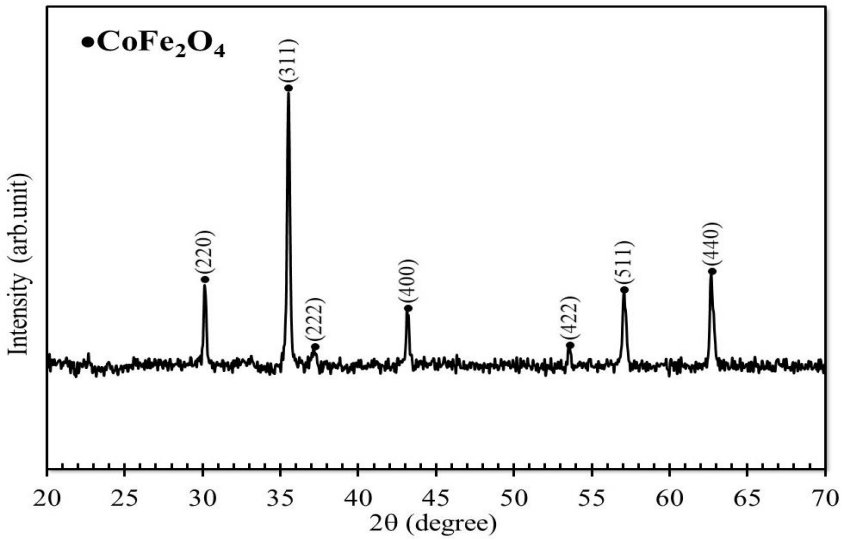

Fig. 2 XRD pattern showing the cobalt ferrite phase

diffractions from (220), (311), (222), (400), (422), (511), and (440) planes of the cobalt ferrite with a cubic spinel structure (JCPDS 22-1086). No impurity phase is detected, confirming that single-phase cobalt ferrite is successfully synthesized by the sol-gel synthesis and subsequent calcination. The crystalline size, evaluated from the XRD peak widths using Scherrer's equation, was approximately 46 nm, but the nanocrystals tend to agglomerate into microclusters.

3.2 Vulcanization characteristics of rubber-cobalt ferrite composites

The cure time corresponding to the cross-linking and the scorch time indicating the processability time, important characteristics of the vulcanization process, are expressed in Fig. 3.

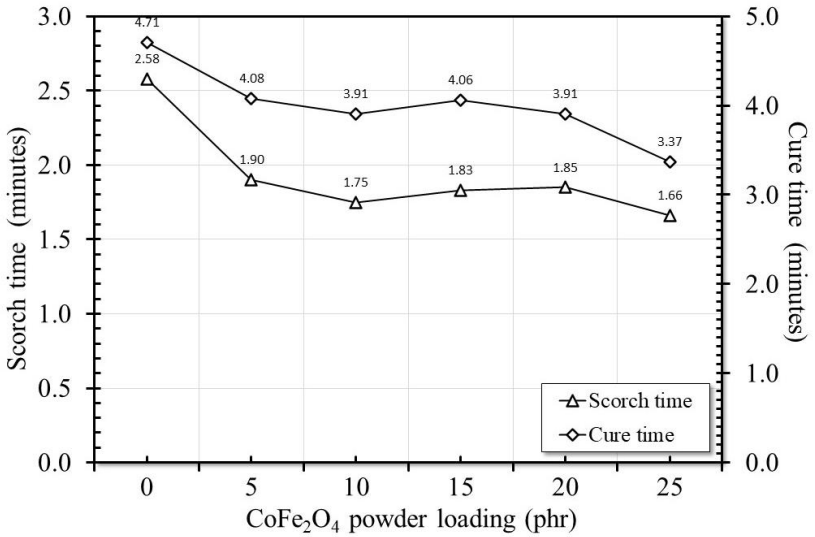

Fig. 3 Scorch time and cure time of rubber composites with varying cobalt ferrite loadings from 0 to 25 phr

Both durations tend to decrease with increasing cobalt ferrite loading from 0 to 25 phr in this study. In the middle range between 10 and 20 phr, slight increases are observed. This trend is due to the interruption of the cross-linking process by ferrite fillers suggested in the literature (Malini *et al.* 2003, Solomon *et al.* 2004, Ismail *et al.* 2007). Interestingly, the vulcanization process in Fig. 3 is significantly shorter than those reported in rubber composites filled with barium ferrite (Solomon *et al.* 2004) and nickel zinc ferrite (Ismail *et al.* 2007).

The minimum torque shown in Fig. 4 is measured by applying the shear stress on the natural rubber before it is completely vulcanized. It indicates the viscosity, which is a ratio of the shear stress to the shear rate. The viscosity of rubber composites is increased with a number of involvement points of the molecular chain and the molecular weight of the rubber. In the process, the viscosity of the rubber composite depends on the mixing time and filler type. An extensive mixing time reduces the viscosity because the molecular rubber chains are torn by shear forces within the mixer. However, these composites were synthesized by blending dry natural rubber sheets for only 10 min. Therefore, the factor influencing the viscosity of the rubber composite should be cobalt ferrite filler. If the fillers are bonded to molecules of rubber-like carbon black or modified clay (Hasan *et al.* 2020), the viscosity of the composite during mixing will be increased. However, non-reinforced cobalt ferrite fillers do not bond with rubber molecules. When cobalt ferrite was added to the compound rubber, the viscosity and hence the minimum torque did not monotonically change with the loading from 5 to 25 phr. The cobalt ferrite fillers act as interrupters reducing the number of involvement points and randomly reducing the minimum torque.

The maximum torque also shown in Fig. 4 indicates elastic properties when vulcanized rubber composites are subjected to a shear force A high maximum torque is due to high modulus (stiffness) of the vulcanizate. Consistent with previous reports on ferrite fillers in natural rubbers (Malini *et al.* 2003, Solomon *et al.* 2004), the increase in maximum torque with the cobalt ferrite loading in this study confirms that the incorporation of the filler reduces the mobility of the macromolecular chains and hence the elasticity of natural rubber matrix.

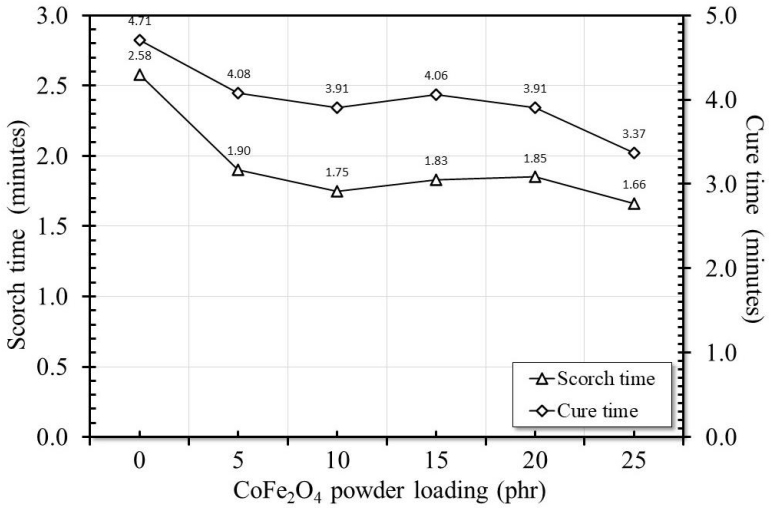

Fig. 4 Maximum and minimum torques of rubber composites with varying cobalt ferrite loadings from 0 to 25 phr

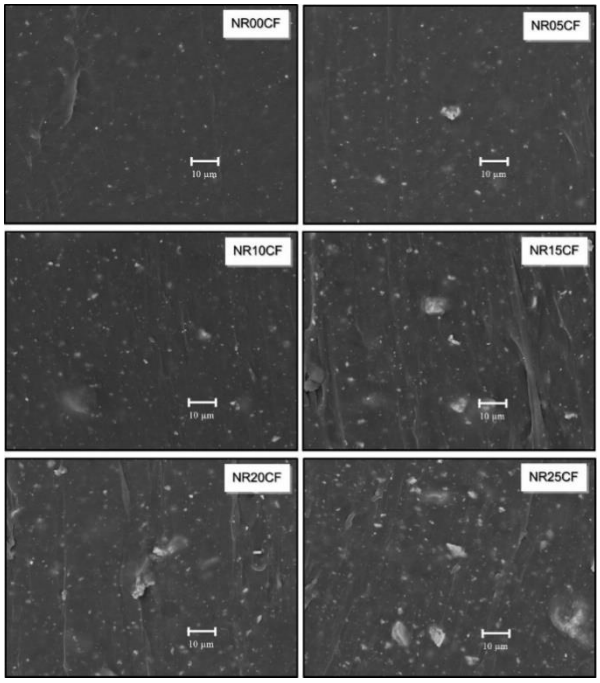

Fig. 5 Morphology of rubber composites with varying cobalt ferrite loadings from 0 to 25 phr

3.3 Surface morphology

From SEM micrographs in Fig. 5, surface morphologies of the rubber composites of varying cobalt ferrite loading are different from the compound rubber (NR00CF). Without ferrite fillers, the surface texture is relatively smooth but appears to have overlapping textures due to sample

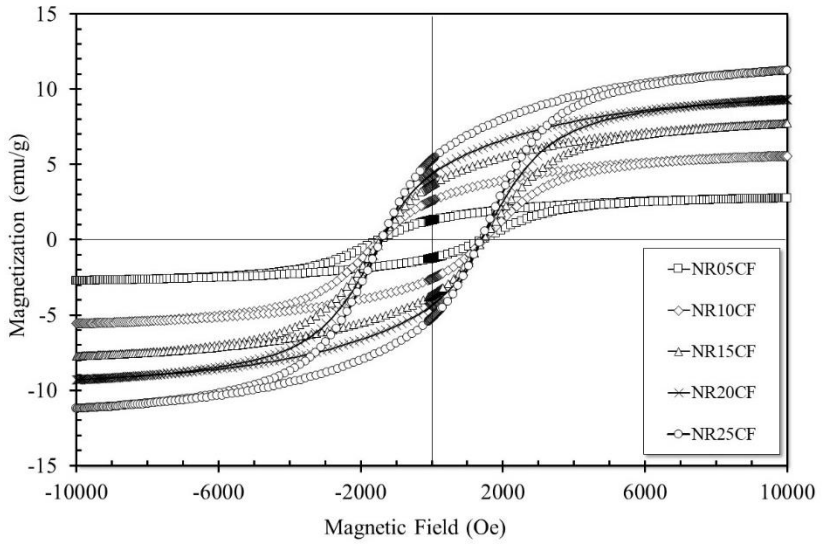

Fig. 6 Hysteresis loops of rubber composites with varying cobalt ferrite loadings from 5 to 25 phr

preparation. The cobalt ferrite clusters are visible even in the case of a minimum 5 phr loading (NR05CF). Some clusters settle in the groove, whereas others are randomly scattered. With increasing loading from 10 to 25 phr, the size of clusters becomes larger than 25 μm, with free volumes also present in the composites. The free volumes increase the porosity, and the roughness of the composites is highly dependent on the cluster size.

3.4 Magnetic hysteresis

Ferrimagnetic properties of the rubber ferrite composites were shown by hysteresis loops in Fig. 6. For every composite, the magnetic field is increased with the applied magnetic field and approaches saturation in the maximum 10 kOe field. The magnetizations and the coercive field from hysteresis loops are shown in Figs. 7 and 8, respectively. Both saturation and remanent magnetizations are linearly increased with increasing cobalt ferrite loading from 0 to 25 phr. The results are consistent with the literature that the saturation magnetization of rubber ferrite composites can be predicted according to the rule of mixture (Malini *et al.* 2001, Solomon *et al.* 2004, Hunyek *et al.* 2013).

On the other hand, the coercive fields of all rubber composites in this study are around 1400 Oe and exhibit only slight reduction with the cobalt ferrite loading. In addition to magnetic anisotropy, the coercive field is sensitive to the stress generated during the fabrication and heat treatment (Malini *et al.* 2001, Solomon *et al.* 2004, Hunyek *et al.* 2013). Fig. 8 also shows the squareness (the ratio of remanence to saturation magnetization) value of 0.46-0.47 because both remanence to saturation magnetization are proportional to the cobalt ferrite loading. The squareness in this range indicates the isotropic alignment of magnetic moments but is larger than those of other natural rubber composites in previous reports (Malini *et al.* 2001, Solomon *et al.* 2004, Hunyek *et al.* 2013). As a control, a VSM measurement on the compound rubber without cobalt ferrite filler (NR00CF) does not yield the hysteresis loop confirming a source of magnetic properties in the composites.

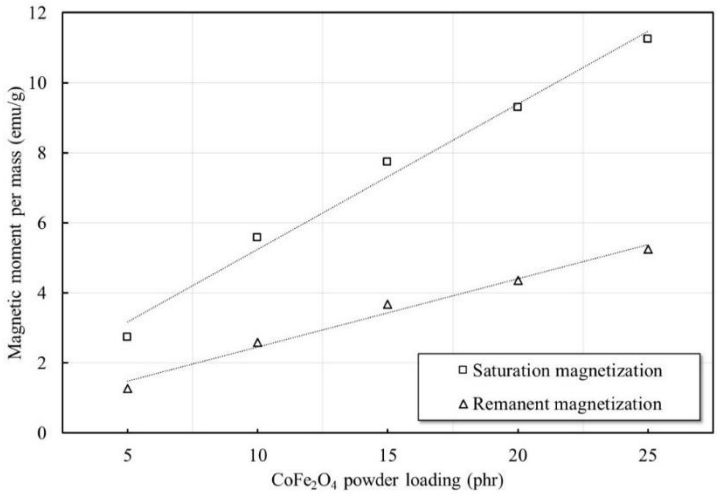

Fig. 7 Saturation and remanent magnetization of rubber composites as a function of cobalt ferrite loadings from 5 to 25 phr

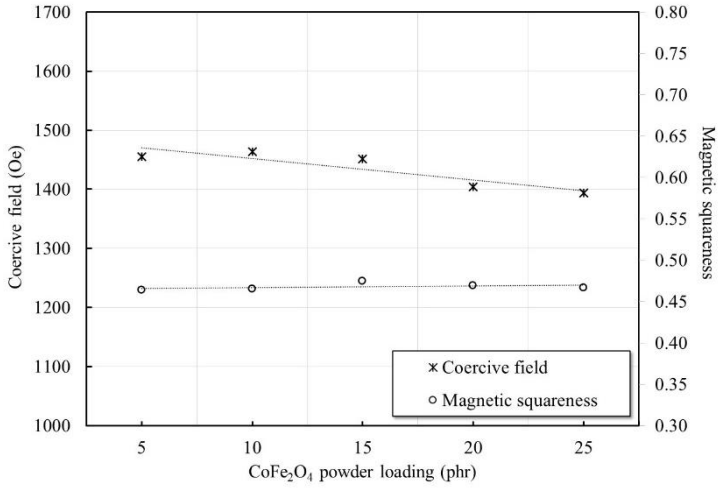

Fig. 8 Coercive field and magnetic squareness of rubber composites as a function of cobalt ferrite loadings from 5 to 25 phr

3.5 Complex permeability and permittivity

In Fig. 9, the complex permeability of rubber ferrite composites is minimal. At 10 MHz, the real part is close to 1 and significantly raised by the loading of 15-25 phr. The imaginary part (magnetic loss) does not exhibit a distinct variation with the loading but clearly increases with the increasing frequency from 10 to 100 MHz. From 100 to 1000 MHz, the complex permeability fluctuates within small regimes. Because the coercive field of cobalt ferrite is substantial, the complex permeability of the composites is significantly influenced by the polymer characteristics. A magnetic loss of greater than 4 was previously reported at 1 MHz in the cobalt ferrite in the polypropylene matrix (Hunyek *et al.* 2019).

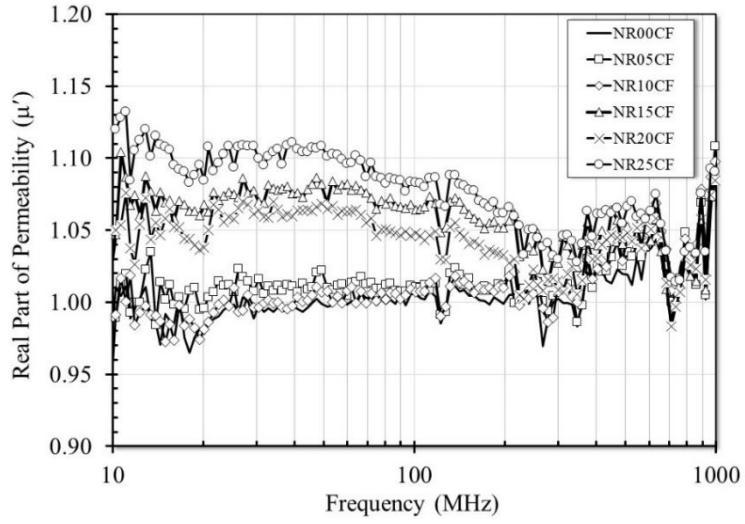

(a)

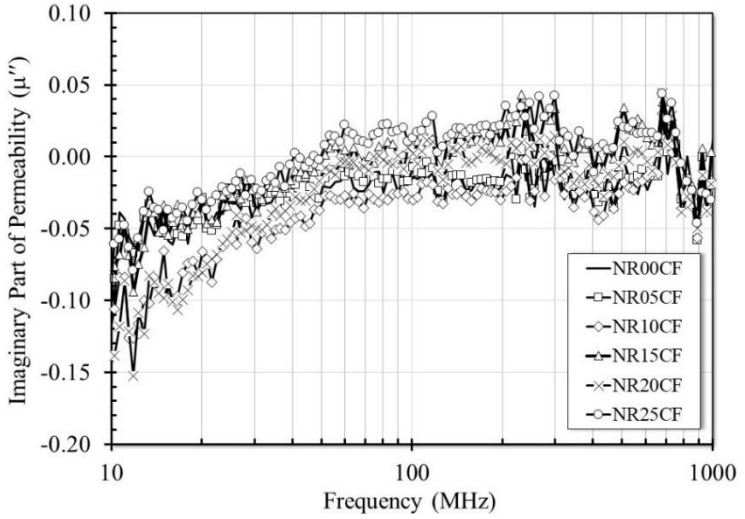

(b)

Fig. 9 Complex permeability of rubber composites with various cobalt ferrite loading as a function of frequency; (a) the real part and (b) the imaginary part

In Fig. 10, the real part of permittivity (dielectric constant) of the rubber compound without cobalt ferrite loading is 2.33 at 10 MHz and reduces to 2.25 at 1000 MHz. Likewise, the imaginary part of permittivity (dielectric loss) is 0.067 at 10 MHz and decreases with frequency to the minimal. The dielectric losses at 10 MHz in other composites containing cobalt ferrites were also below 0.4 (Hunyek *et al.* 2013, Hunyek *et al.* 2019). At higher frequencies, fluctuations of complex permittivity observed in all rubber ferrite composites, as well as the control (NR00CF) and previous measurements (Hunyek *et al.* 2013), are seemingly caused by the parasitic effect of the test fixtures. At every frequency, the complex permittivity increases with increasing cobalt ferrite loading from 5 to 25 phr. It can be explained by the effect of frequency on the relaxation

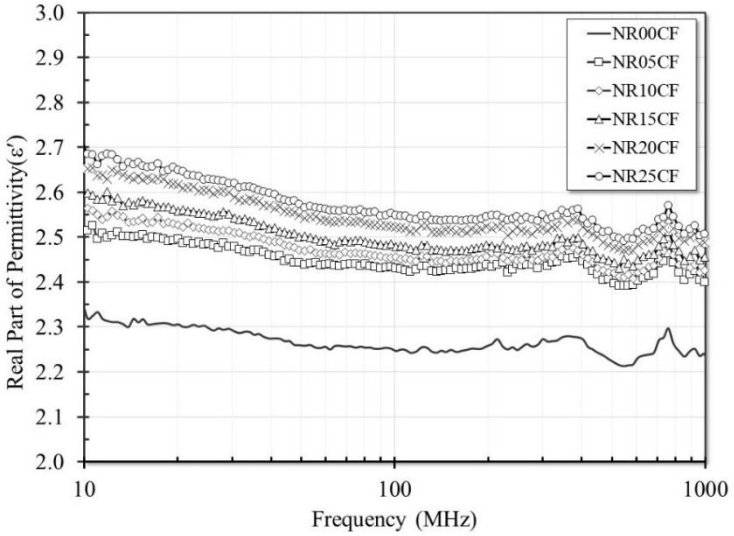

(a)

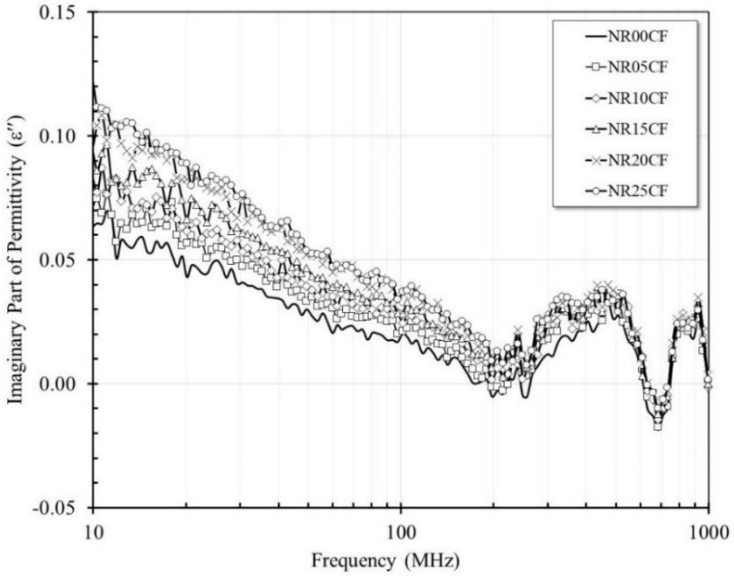

(b)

Fig. 10 Complex permittivity of rubber composites with various cobalt ferrite loading as a function of frequency; (a) the real part and (b) the imaginary part

time of the polarization reversal and the Maxwell-Wagner effect, in which the permittivity of composites is regulated by surface charges of the fillers induced during the polarization (Borah and Bhattacharyya 2012). The permittivity of the rubber composites was dependent on the cobalt ferrite loading due to the accumulation of surface charges. The preparation of composites by the internal mixer technique results in negligible porosity and unlikely affects the charge accumulation.

The modest dielectric and magnetic losses limit the high-frequency use of these rubber ferrite

composites. The values can be enhanced in the microwave regime by incorporating cobalt ferrites into graphite (Ismail *et al.* 2019), graphene (Zhang *et al.* 2019), single-walled or multi-walled carbon nanotubes (Wang *et al.* 2019, Khan *et al.* 2020). Multiple interfaces in the nanocomposites are beneficial for electromagnetic wave shielding (Wang *et al.* 2021b). Such a characteristic could be enhanced in the form of a laminated structure (He *et al.* 2022).

4. Conclusions

Cobalt ferrite powders, synthesized by the sol-gel method using tapioca starch as a cheating agent and then calcined at 600°C, were incorporated into natural rubber compounds in an internal mixer. The properties of the natural rubber composites with 5-25 phr cobalt ferrite are summarized as follows.

1) The loading of cobalt ferrite into natural rubber tends to reduce both cure and scorch times. Some cobalt ferrite particles were clustered together and randomly dispersed in the rubber matrix.

2) The remanent and saturation magnetizations are proportional to the cobalt ferrite loading.

3) The complex permeability at 10-1000 MHz is minimal. The complex permittivity increases due to the accumulation of surface charge with increasing loading of cobalt ferrite fillers. By raising the frequency from 10 MHz to 1000 MHz, the real and imaginary parts tend to reduce.

Acknowledgments

The research described in this paper was financially supported by the National Science and Technology Development Agency (Grant no. P-18-51764) and Rajamangala University of Technology Rattanakosin (Grant no. FDA-CO-62-8904-TH). The authors would like to thank Dr. P. Jantaratana of Kasetsart University for the access to characterization facilities.

References

Abou Hammad, A.B., Abd El-Aziz, M.E., Hasanin, M.S. and Kamel, S. (2019), "A novel electromagnetic biodegradable nanocomposite based on cellulose, polyaniline, and cobalt ferrite nanoparticles", *Carbohydr. Polym*., **216**, 54-62. https://doi.org/10.1016/j.carbpol.2019.03.038.

Borah, K. and Bhattacharyya, N.S. (2012), "Magnetodielectric composite with ferrite inclusions as substrates for microstrip patch antennas at microwave frequencies", *Compos. Part B: Eng*., **43**, 1309-1314. https://doi.org/10.1016/j.compositesb.2011.11.067.

Das, T. and Verma, B. (2019), "High performance ternary polyaniline-acetylene black-cobalt ferrite hybrid system for supercapacitor electrodes", *Synth. Met*., **251**, 65-74. https://doi.org/10.1016/j.synthmet.2019.03.025.

Garigipati, R.K.S. and Malkapuram, R. (2020), "Sawdust reinforced polybenzoxazine composites: Thermal and structural properties", *Adv. Mater. Res*., **9**(4), 311-321. https://doi.org/10.12989/amr.2020.9.4.311.

Hasan, A., Aznury, M., Purnamasari, I., Manawan, M. and Liza, C. (2020), "Curing characteristics and physical properties of natural rubber composites using modified clay filler", *Int. J. Technol*., **11**(4), 830-841. https://doi.org/10.14716/ijtech.v11i4.4083.

He, Q.M., Tao, J.R., Yang, Y., Yang, D., Zhang, K., Fei, B. and Wang, M. (2022), "Electric-magnetic-

dielectric synergism and Salisbury screen effect in laminated polymer composites with multiwall carbon nanotube, nickel, and antimony trioxide for enhancing electromagnetic interference shielding", *Compos. Part A: Appl. Sci. Manuf.*, **156**, 106901. https://doi.org/10.1016/j.compositesa.2022.106901.

Hunyek, A., Sirisathitkul, C., Mahaphap, C., Boonyang, U. and Tangwatanakul, W. (2017), "Sago starch: Chelating agent in sol-gel synthesis of cobalt ferrite nanoparticles", *J. Australian Ceram. Soc*., **53**, 173-176. https://doi.org/10.1007/s41779-017-0022-1.

Hunyek, A., Sririsathitkul, C. and Jantaratana, P. (2013), "Magnetic and dielectric properties of natural rubber and polyurethane composites filled with cobalt ferrite", *Plast. Rubb. Compos*., **42**, 89-92. https://doi.org/10.1179/1743289812Y.0000000003.

Hunyek, A., Sririsathitkul, C. and Jantaratana, P. (2019), "Comparative electromagnetic properties of polypropylene composites loaded with cobalt ferrites by melt mixing", *Int. J. Nanoelectron. Mater*., **12**(4), 459-466.

Ismail, H., Sam, S.T., Mohd Noor, A.F. and Bakar, A.A. (2007), "Properties of ferrite-filled natural rubber composites", *Polym. Plast. Technol. Eng*., **46**, 641-650.

Ismail, I., Matori, K.A., Abbas, Z., Zulkimi, M.M.M., Idris, F.M., Zaid, M.H.M., Rahim, N., Hasan, I.H. and Song, W.H. (2019), "Single- and double-layer microwave absorbers of cobalt ferrite and graphite composite at gigahertz frequency", *J. Supercond. Nov. Magn*., **32**, 935-943. https://doi.org/10.1007/s10948-018-4749-x.

Jauhar, S., Kaur, J., Goyal, A. and Singhal, S. (2016), "Tuning the properties of cobalt ferrite: A road towards diverse applications", *RSC Adv*., **6**, 97694. https://doi.org/10.1039/C6RA21224G.

Kalmagambetova, A. and Bogoyavlenskaya, T. (2021), "Effect of physical properties of samples on the mechanical characteristics of high-density polyethylene (HDPE)", *Adv. Mater. Res*., **10**(1), 67-76. https://doi.org/10.12989/amr.2021.10.1.067.

Khalifa, S.B., Gassoumi, M., Dhahbi, A.B., Alresheedi, F., Mahmoud, A.Z.A. and Beji, L. (2020), "The effect of the cobalt ferrites nanoparticles ($CoFe_2O_4$) on the porous silicon deposited by spin coating", *Alex. Eng. J*., **59**, 1093-1098. https://doi.org/10.1016/j.aej.2019.12.031.

Khan, L.U., Younas, M., Khan, S.U. and Ur Rehman, M.Z. (2020), "Synthesis and characterization of $CoFe_2O_4$/MWCNTs nanocomposites and high-frequency analysis of their dielectric properties", *J. Mater. Eng. Perform*., **29**, 251-258. https://doi.org/10.1007/s11665-020-04572-9.

Kumar, M., Shankar, S., Tuli, V., Mittal, S., Joshi, V., Jha, M.K. and Gupta, G. (2020), "Structural analysis and magnetoelectric sensing in cobalt ferrite-$BaTiO_3$ composites", *Nat. Acad. Sci. Lett*., **43**(7), 677-679. https://doi.org/10.1007/s40009-020-00939-7.

Mahalakshmi, S., Jayasri, R., Nithiyanatham, S., Swetha, S. and Santhi, K. (2019), "Magnetic interactions and dielectric behaviour of cobalt ferrite and barium titanate multiferroics nanocomposites", *Appl. Surf. Sci*., **494**, 51-56. https://doi.org/10.1016/j.apsusc.2019.07.096.

Malini, K.A., Kurian, P. and Anantharaman, M.R. (2003), "Loading dependence similarities on the cure time and mechanical properties of rubber ferrite composites containing nickel zinc ferrite", *Mater. Lett*., **57**, 3381-3386. https://doi.org/10.1016/S0167-577X(03)00079-X.

Malini, K.A., Mohammed, E.M., Sindhu, S., Kurian, P., Date, S.K., Kulkarni, S.D., Joy, P.A. and Anantharaman, M.R. (2001), "Magnetic and processability studies on rubber ferrite composites based on natural rubber and mixed ferrite", *J. Mater. Sci*., **36**, 5551-5557. https://doi.org/10.1023/A:1012545127918.

Megahed, M., Tobbala, D.E. and Abd El-baky, M.A. (2021), "The effect of incorporation of hybrid silica and cobalt ferrite nanofillers on the mechanical characteristics of glass fiber-reinforced polymeric composites", *Polym. Compos*., **42**(1), 271-284. https://doi.org/10.1002/pc.25823.

Mirzaee, S., Shayesteh, S.F. and Mahdavifar, S. (2014), "Synthesis and characterization of cubic omega-3-coated cobalt ferrite nanoparticles", *J. Supercond. Nov. Magn*., **27**, 1781-1785. https://doi.org/10.1007/s10948-014-2512-5.

Mmelesi, O.K., Masunga, N., Kuvarega, A., Nkambule, T.T., Mamba, B.B. and Kefeni, K.K. (2021), "Cobalt ferrite nanoparticles and nanocomposites: Photocatalytic, antimicrobial activity and toxicity in water treatment", *Mater. Sci. Semicond. Proc.*, **123**, 105523. https://doi.org/10.1016/j.mssp.2020.105523.

Mustafa, G., Islam, M.U., Zhang, W., Anwar, A.W., Jamil, Y., Murtaza, G., Ali, I., Hussain, M., Ali, A. and Ahmad, M. (2015), "Influence of the divalent and trivalent ions substitution on the structural and magnetic properties of $Mg_{0.5-x}Cd_xCo_{0.5}Cr_{0.04}Tb_yFe_{1.96-y}O_4$ ferrites prepared by sol-gel method", *J. Magn. Magn. Mater*., **387**, 147-154. http://doi.org/10.1016/j.jmmm.2015.03.091.

Ojogbo, E., Blanchard, R. and Mekonnen, T. (2018), "Hydrophobic and melt processable starch-laurate esters: Synthesis, structure-property correlations", *J. Polym. Sci. Part A: Polym. Chem*., **56**(6), 2611-2622. https://doi.org/10.1002/pola.29237.

Paluch, M., Ostrowska, J., Tyński, P., Sadurski, W. and Konkol, M. (2022), "Synthesis and characterization of cubic omega-3-coated cobalt ferrite nanoparticles", *J. Polym. Environ*., **30**, 728-740. https://doi.org/10.1007/s10924-021-02235-x.

Shapkin, N.P., Panasenko, A.E., Khal'chenko, I.G., Pechnikov, V.S., Maiorov, V.Y., Maslova, N.V., Razov, V.I. and Papynov, E.K. (2020), "Magnetic composites based on cobalt ferrite, vermiculite, and rice husks: Synthesis and properties", *Russian J. Inorg. Chem*., **65**(10), 1614-1622. https://doi.org/0.1134/S0036023620100186.

Shariati, A., Ebrahimi, F., Karimiasl, M., Selvamani, R. and Toghroli A. (2020), "On bending characteristics of smart magneto-electro-piezoelectric nanobeams system", *Adv. Nano Res*., **9**(3), 183-191. https://doi.org/10.12989/anr.2020.9.3.183.

Solomon, M.A., Kurian, P., Joy, P.A. and Anantharaman, M.R. (2004), "Processability and magnetic properties of rubber ferrite composites containing barium ferrite", *Int. J. Polym. Mater*., **53**, 565-575. https://doi.org/10.1080/00914030490461685.

Srinivasan, S.Y., Paknikar, K.M., Bodas, D. and Gajbhiye, V. (2018), "Applications of cobalt ferrite nanoparticles in biomedical nanotechnology", *Nanomedicine*, **13**(10), 1221-1238. https://doi.org/10.2217/nnm-2017-0379.

Wang, M., Tang, X.H., Cai, J.H., Wu, H., Shen, J.B. and Guo, S.Y. (2021a), "Construction, mechanism and prospective of conductive polymer composites with multiple interfaces for electromagnetic interference shielding: A review", *Carbon*, **177**, 377-402. https://doi.org/10.1016/j.carbon.2021.02.047.

Wang, M., Zhang, Y., Dong, C., Chen, G., Guan, H. (2019), "Preparation and electromagnetic shielding effectiveness of cobalt ferrite nanoparticles/carbon nanotubes composites", *Nanomater. Nanotechnol*., **9**, 1-7. https://doi.org/10.1177/1847980419837821.

Wang, Y., Gao, Y.N., Yue, T.N., Chen, X.D. and Wang, M. (2021b), "Achieving high-performance and tunable microwave shielding in multi-walled carbon nanotubes/polydimethylsiloxane composites containing liquid metals", *Appl. Surf. Sci*., **563**, 150255. https://doi.org/10.1016/j.apsusc.2021.150255.

Yang, Y., Ali, F., Said, A., Ali, N., Ahmad, S., Raziq, F. and Khan, S. (2021), "Fabrication, mechanical, and electromagnetic studies of cobalt ferrite based-epoxy nanocomposites", *Polym. Compos*., **42**(1), 285-296. https://doi.org/10.1002/pc.25824.

Zeng, Y., Zhu, X., Xie J. and Chen, L. (2021), "Ionic liquid coated magnetic core/shell $CoFe_2O_4$@SiO_2 nanoparticles for the separation/analysis of trace gold in water sample", *Adv. Nano Res*., **10**(3), 295-312. https://doi.org/10.12989/anr.2021.10.3.295.

Zhang, N., Liu, X.D., Huang, Y., Wang, M.Y., Li, S.P., Zong, M. and Liu, P.B. (2019), "Novel nanocomposites of cobalt ferrite covalently-grafted on graphene by amide bond as superior electromagnetic wave absorber", *J. Colloid Interf. Sci*., **540**, 218-227. https://doi.org/10.1016/j.jcis.2019.01.025.

CC